

Accuracy of RT code SORD for realistic atmospheric profiles

Sergey Korkin^{*a,b}, Alexei Lyapustin^b, Aliaksandr Sinyuk^{c,b}, and Brent Holben^b

^aUSRA GESTAR, 7178 Columbia Gateway Drive, Columbia, MD, USA 21046; ^bNASA GSFC, 8800 Greenbelt Rd., Greenbelt, MD, USA 20771; ^cSigma Space Corp., 4600 Forbes Blvd., Lanham-Seabrook, MD USA 20706

ABSTRACT

We discuss accuracy of our recently developed RT code SORD using 2 benchmark scenarios published by the IPRT group in 2015. These scenarios define atmospheres with a complicate dependence of scattering and absorption properties over height (profile). Equal step, $dh=1\text{km}$, is assumed in the profiles. We developed subroutines that split such atmospheres into layers of the same optical thickness, $d\tau$. We provide full text of the subroutines with comments in Appendix. The $d\tau$ is a step for vertical integration in the method of successive orders. Modification of the input profiles from “equal step over h ” to “equal step over τ ” changes input for RT simulations. This may cause errors at or above the acceptable level of the measurement uncertainty. We show errors of the RT code SORD for both intensity and polarization. In addition to that, using our discrete ordinates RT code IPOL, we discuss one more IPRT scenario, in which changes in height profile indeed cause unacceptable errors. Clear understanding of source and magnitude of these errors is important, e.g. for the AERONET retrieval algorithm.

SORD is available from http://maiac.gsfc.nasa.gov/pub/skorkin/SORD_IP_16B/ or by email request from the first author.

Keywords: RT code, successive orders, polarization, height profiles, accuracy assessment

1. INTRODUCTION

Recently we announced and carefully tested new successive orders (SO) of scattering^{1,2} radiative transfer (RT) code SORD³, which now works as part of the AERONET⁴ retrieval algorithm⁵. The code showed high accuracy in a variety of published scenarios, including most benchmarks from the recent International working group on Polarized Radiative Transfer (IPRT) codes intercomparison⁶. Nevertheless, we did not discuss accuracy of SORD in three IPRT benchmarks. These scenarios use complicate height distribution (profile) for scattering and absorption optical properties of atmosphere.

The method of successive orders uses numerical integration over vertical optical thickness, τ . Often one integrates with an equal step, $d\tau^{7,8}$. This requires splitting the total (scattering+absorption) profile of optical thickness, τ , into $d\tau$ -thick “microlayers”. In order to compute the single scattering albedo (SSA) for each microlayer, the original profile of scattering optical thickness is also redistributed over height, h . Because of that, the $SSA(h)$ profile in the actual numerical simulation differs from the original one. Depending on a particular case, this may or may not cause significant deviation from the benchmark. For example, when $SSA(\tau)$ is known analytically, we have reported³ perfect agreement with the published numbers⁹. In this case, naturally, the smaller is the integration step $d\tau$ the better is the agreement.

As opposed to that, the IPRT case B4 defines a scenario with three optical layers over ocean. Cloud of the total optical thickness 5 is mixed with Rayleigh scattering layer of thickness 0.002. Pure Rayleigh scattering layers of thickness 0.014 and 0.005 bound the cloud-Rayleigh mixture on top and bottom, respectively. Thus, the total Rayleigh optical thickness is 0.021 (800 nm band), which is much thinner than the cloud. Despite this difference, Rayleigh cannot be totally ignored (see examples below). Moreover, mixing all the Rayleigh and cloud in a single optical layer (good for numerical simulations) gives up to 1% deviation from the benchmark for intensity observed within 60 degrees from the surface normal, and up to 4% from radiation detected within 80 degrees. These numbers obtained with our discrete ordinates (DO) RT code IPOL, which showed high accuracy in the mentioned IPRT codes intercomparison⁶. The method of discrete ordinates integrates over optical thickness analytically. This allows to accurately account for arbitrary scattering profile, though at the expense of run-time. Hence, all the mentioned deviation from benchmark is due to tiny change of the vertical scattering profile.

On the contrary, for a realistic case of dust-Rayleigh-gas (absorption) mixture (IPRT case B3) as well as for Rayleigh-gas mixture (IPRT case B2), the new RT code SORD deviates from the published numbers by no more than 0.05%

^{*}sergey.v.korkin@nasa.gov

(averaged over all view directions; same level of error for intensity and degree of linear polarization). In the Appendix we give full text of subroutines that compute profiles with equal step dt from the original profiles with equal step dh , km. We must note here that no successive orders of scattering RT codes participated in the 2015 IPRT intercomparison. Hence, accuracy of the SO codes in these cases remained unknown.

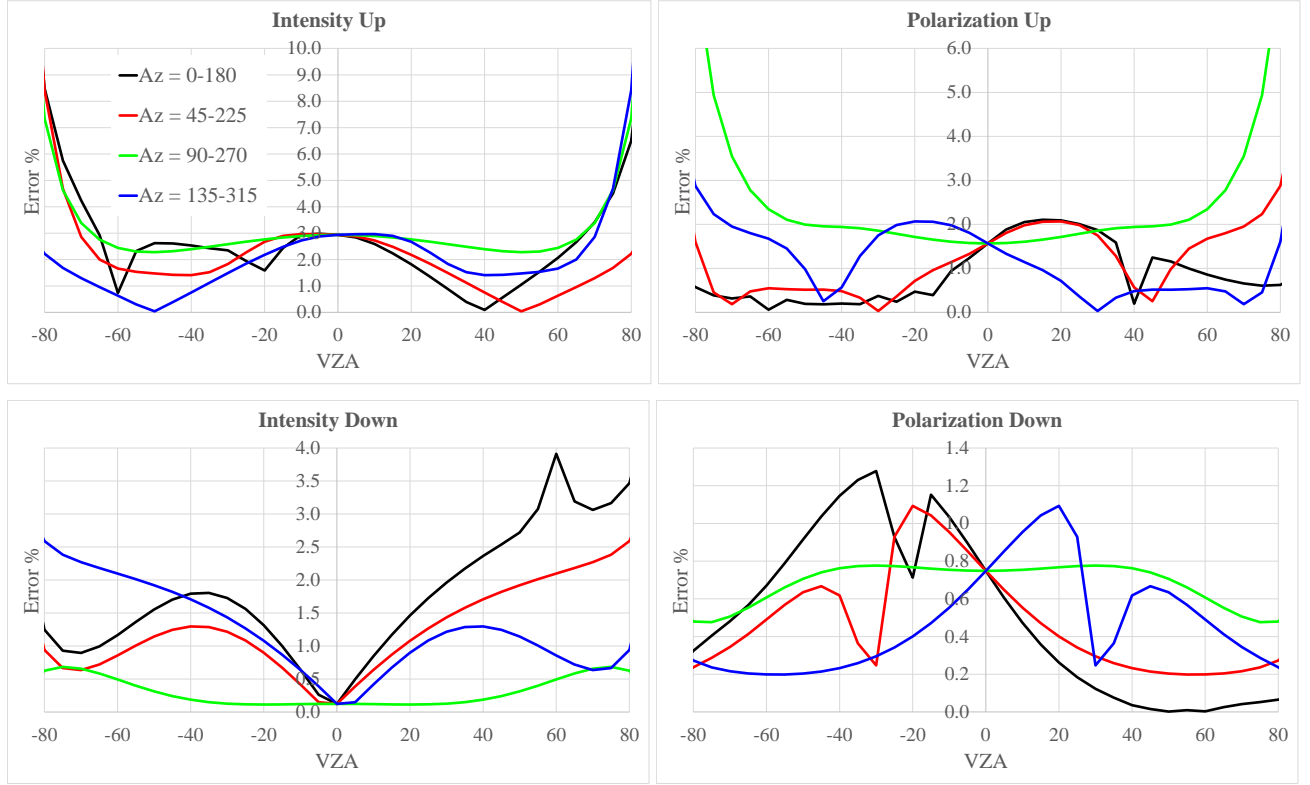


Figure 1. Relative deviation between RT simulation for an exact Cloud-Rayleigh scenario, and RT simulation in case when Rayleigh is ignored ($\tau_c/\tau_R \sim 250$). The Figure shows results for reflected (up) and transmitted (down) intensity and polarization at several meridional planes.

Below we discuss details of comparison of SORD against accurate results generated with our code IPOL, which proved high accuracy in all the IPRT tests. We analyze two relative errors. One is for the total intensity, I . Another is for the degree of linear polarization,

$$P = \sqrt{Q^2 + U^2} / I, \quad 0 \leq P \leq 1. \quad (1)$$

For the I , the relative error between the benchmark, I_B , and SORD, I_S , is defined by absolute value

$$\delta I = 100\% \cdot |I_B - I_S| / I_B. \quad (2)$$

For the P , we use the following definition

$$\delta P = 100\% \cdot |P_B - P_S|, \quad (3)$$

where P_B and P_S are degree of linear polarization, Eq.(1), for benchmark and SORD, respectively. We use % in Eq.(3) for consistency with Eq.(2). For example, for $P_B = 0.13 = 13\%$ and $P_S = 0.12 = 12\%$, one gets $\delta P = 1\%$. As follows from Eqs. (2) and (3), we skip the sign.

Finally, we must define some level of sufficient accuracy for I and P . For that, we refer the reader to Table 1 from Diner et al.¹⁰ (see p.8429). The table shows polarimetric uncertainty for several space borne instruments: Polarization and Directionality of Earth's Reflectances (POLDER) - 2%; Multiangle SpectroPolarimetric Imager (MSPI) - 0.5%; Aerosol Polarimeter Sensor (APS) - 0.2%. Hasekamp and Langgraf¹¹ (see Conclusion, p.3343) set the same requirement 0.002 =

0.2% for the relative Stokes parameters, $q = Q/I$ and $u = U/I$, and no more than 1% for the intensity, I . In the discussion below, we assume 1% and 0.2% to be satisfactory level of error of numerical simulation of intensity and degree of linear polarization, respectively. Further on we refer to the degree of linear polarization as “polarization” for simplicity.

2. ACCURACY ASESMENT

2.1 Cloud and Rayleigh mixture over ocean

In this paragraph, we focus on the IPRT case B4: Standard atmosphere with Rayleigh scattering, cloud of water droplets and underlying ocean surface. The cloud layer is located between 2 and 3km. At $\lambda=800\text{nm}$, the cloud phase function peak value is about 3600, average scattering cosine is about 0.86, $K=500$ Legendre coefficients, cloud optical thickness $\tau_c = 5.0$, and SSA equals 0.999979. We refer the reader to Figure 2 in the IPRT paper⁶. The figure shows all elements of the cloud phase matrix. Solar zenith angle 60 degrees is assumed.

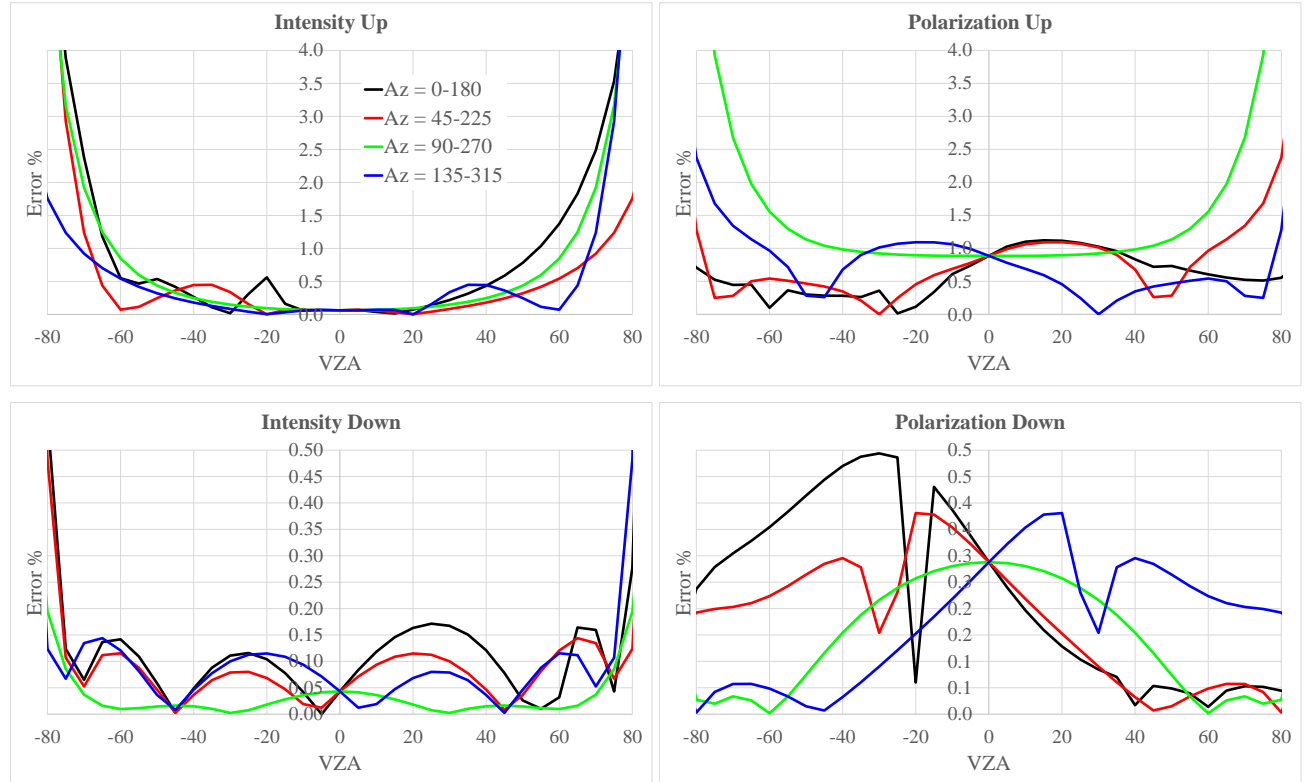


Figure 2. Same as in Figure 1, except for Rayleigh and cloud mixed in a single layer.

At $\lambda=800\text{nm}$, the total Rayleigh optical thickness, τ_R , equals 0.002098185. In the case B4, the Rayleigh atmosphere is defined with 30 layers from 0 to 30 km with 1 km step. However, without gas absorption, the Rayleigh atmosphere can be defined with only 3 layers: above the cloud, mixed with the cloud within 2-3 km, and below cloud. From top to bottom, Rayleigh optical thicknesses of each layer are $\tau_{R1} = 0.01445613$ (above 3 km), $\tau_{R2} = 0.001962413$ (between 3 and 2 km), and $\tau_{R3} = 0.004563307$ (below 2km). We keep the same number of significant digits as defined in the benchmark.

This scenario is inconvenient for both methods, DO and SO, if one seeks for a fast simulation. The SO converges relatively slow in case of thick cloudy atmospheres (more than 5.0 in this case), while the DO relies on singular value decomposition in each of the three layers and several matrix multiplications and inversions to couple the layers and the surface¹². Reduction of the number of optical layers by modifying the height profile obviously helps to accelerate simulation. Further, we analyze how minor changes in the Rayleigh scattering height profile affects the result of RT simulation. In this section, we used our DO code IPOL that proved high accuracy in the recent RT codes intercomparison⁶. All errors shown below are due to changes in profile, and not to accuracy of the RT code IPOL.

Given the fact that $\tau_R \ll \tau_C$, and both cloud and Rayleigh scattering are conservative, it seems natural to neglect Rayleigh and simulate RT in a cloud over ocean. Figure 1 shows results of accuracy analysis for the case. In this Figure, we show relative error between exact result for 3 layers⁶, and the cloud-over-ocean model for reflected (top row) and transmitted (bottom row) radiation. Left and right columns show errors for total intensity and polarization, respectively. Positive values of view zenith angles (VZA) correspond to relative azimuth $Az = 0, 45, 90, 135$. Negative values correspond to $Az+180^\circ$ (whole meridional plane of observation). Black line, $Az=0-180$, is the principal plane. As expected, result for $Az=90-270$ (green line) is symmetric with respect to Y-axis. Results for $Az=45-225$ and $135-315$ are mirror images of each other. As one can see from the figure and the level of acceptable error (see Introduction), Rayleigh scattering cannot be completely ignored in this case despite that $COT/ROT \sim 250$.

The next possible assumption would be to ignore Rayleigh height profile and mix the whole Rayleigh and cloud in a single layer. In this case, the DO RT codes computes singular value decomposition only once. In addition to that, it does not need to couple several layers in atmosphere using matrix multiplications and inversion (one per each coupled layers). Figure 2 shows errors for the case. This scenario definitely better fits the benchmark, but still the error either at or above acceptable level of 0.5% - 1.0%.

Figures 3 shows results for a 2-layers model. In this model, pure Rayleigh with $\tau_{R1}=0.01445613$ is on top (above 3km), while the rest of Rayleigh and the cloud are mixed in the bottom layer. Results are satisfactory for both reflected and transmitted intensity and polarization.

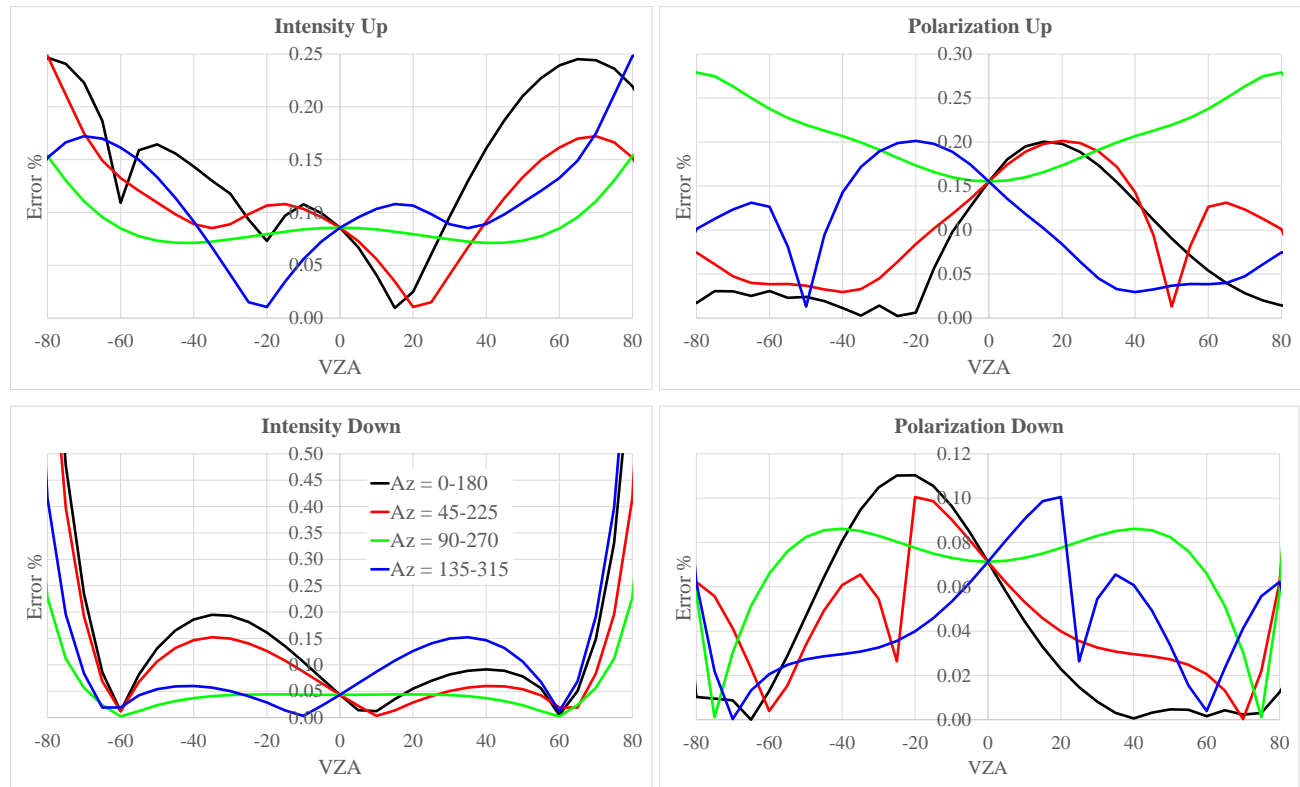


Figure 3. Same as in Figure 2 except for a model with two layers. Rayleigh layer from the IPRT-B4 case is on top.

Finally, Figure 4 shows another 2-layers model: pure Rayleigh with $\tau_{R3}=0.004563307$ as the bottom layer, while the top layer is a mixture of Rayleigh and cloud. One can see poor accuracy for reflected and satisfactory result for transmitted radiation.

From Figures 1-4, we derive several important conclusions. Rayleigh scattering plays important role in radiative transfer even if $\tau_C/\tau_R = 250$. If we neglect the Rayleigh scattering completely, the resulting error exceeds its acceptable level. Mixing all the Rayleigh and cloud in the same layer improves accuracy of simulations, but does not solve the problem entirely. For reflected polarization, for example, the error remains way above the desired 0.2%. For satellite remote sensing of atmosphere, it seems natural to use a model with 2 layers with Rayleigh on top. In this case, the reflected

intensity and polarization are at the desired level of accuracy. Noteworthy that the same “Rayleigh on top” model seems to work better for the AERONET-type systems as well. The “Rayleigh on bottom” model shows on average higher levels of error.

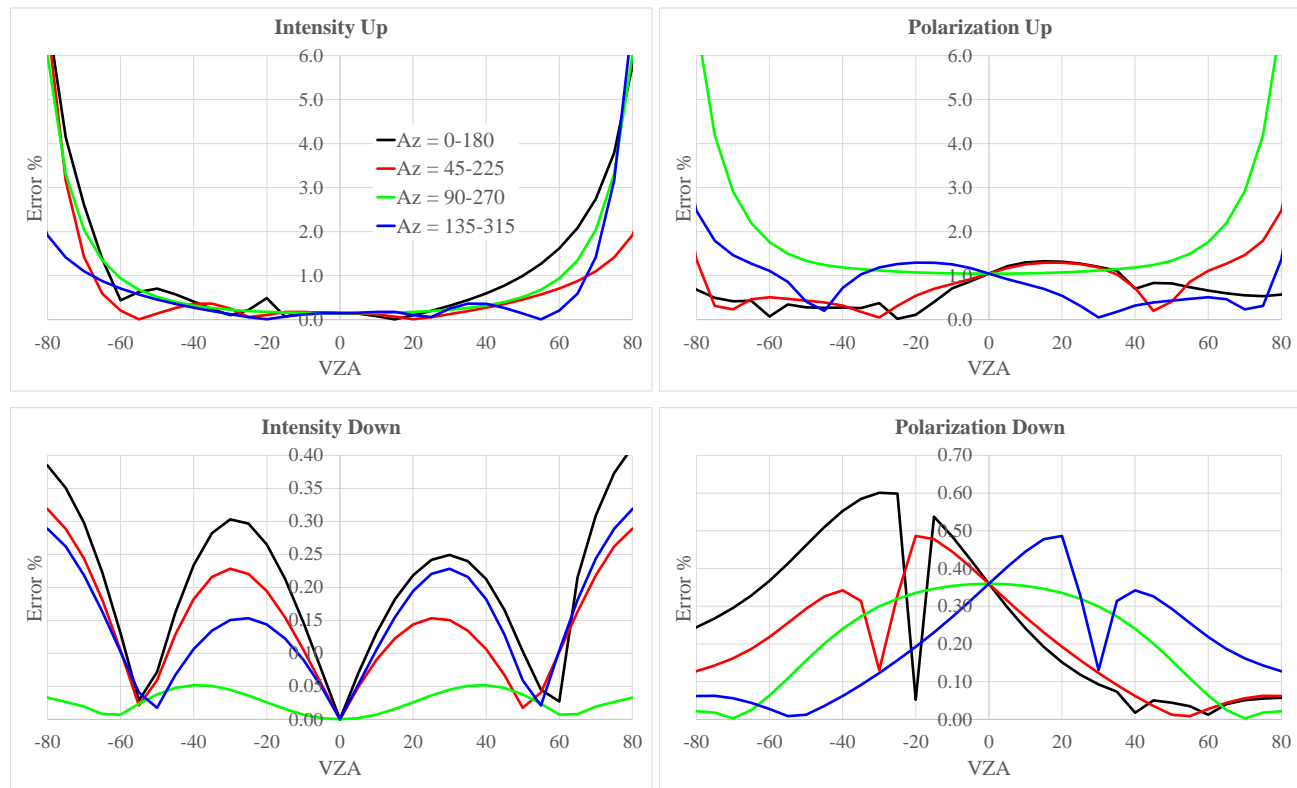


Figure 4. Same as in Figure 3, except for Rayleigh scattering layer from the IPRT-B4 case is below the cloud.

We judged the errors based on the measurement requirements. In order not to be a bottleneck in the data processing algorithm, RT code developers must guarantee better accuracy. We used 0.1% for both intensity and polarization in our recent paper about RT code SORD³, 0.05% is considered a good agreement in the recent IPRT paper⁶ (see Conclusion). None of the results shown in Figure 1-4 met the criterion. This leaves us with important question: if tiny change in the Rayleigh scattering profile is important, what is the accuracy of the SO RT codes in case of realistic multi-layer profiles? Since none of the SO codes participated in the recent IPRT RT codes intercomparison, we study accuracy of our code SORD in the IPRT cases B2 and B3. We discuss these our results in the next Section.

2.2 Successive orders RT code and cases with multi-layer height profiles

In this Section, we compare our code SORD against IPRT benchmark scenarios B2: Rayleigh scattering and molecular absorption and B3: Aerosol profile. In other words, case B2 correspond to height-dependent single scattering albedo and the same Rayleigh scattering law. In B3 not only SSA, but ratio between Rayleigh and aerosol scattering also varies with height.

Figure 5 shows Rayleigh (blue), gas (black), aerosol (orange), and total (red) height profiles defined with equal step 1km over height, from 0km to 30km. As discussed above, the SO method often requires splitting atmosphere with an equal step over optical thickness. This results in some change of optical properties of atmosphere. Here we analyze the influence of this change on the result of numerical simulation of radiative transfer.

We start with the IPRT case B2. Rayleigh scattering profile is shown in Figure 5, blue line. This profile means that, for example, Rayleigh scattering optical thickness from 30km to 10km is close to 0.2. Total Rayleigh scattering optical depth from 30km to 0 km is about 0.85. Gas absorption optical thickness, black line in Figure 5 (right), also depends on height. We solve the problem of using of the given profiles in the RT code SORD in two steps. At the first step, we split the total (Rayleigh + gas) optical thickness with an equidistant step over optical thickness using subroutine `SPLITTAU`

(see Appendix for the subroutine full text). On output of this subroutine, we have an array of heights, XKM , that splits atmosphere into pieces of equal optical thicknesses. On the second step, we recompute (regroup) the Rayleigh scattering optical thickness from the initial ZKM (1km step) to XKM using subroutine `GROUPTAU` (we also give full text of this subroutine in the Appendix). With the new array of scattering optical depths between elements of XKM , we compute SSA for each new optical layer and run the RT code as usual. Figure 6 shows that results of RT simulation in the atmosphere with modified scattering optical properties does not differ much from the ones computed for the original atmosphere. All errors for intensity and polarization are within the desired accuracy for both reflected and transmitted intensity and polarization.

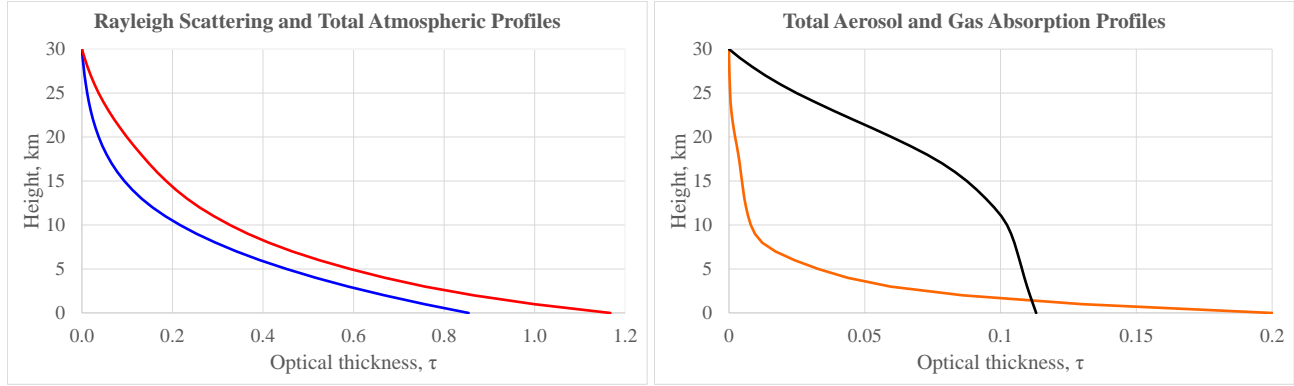


Figure 5. Profiles of optical thickness. Left figure: Rayleigh scattering (blue) for the IPRT cases B2 and B3, and total atmospheric profile (red) for the case IPRT B3 only. Right figure: gas absorption profile (black) for the IPRT cases B2 and B3, and total (scattering + absorption) aerosol profile (orange) for the IPRT case B3 only.

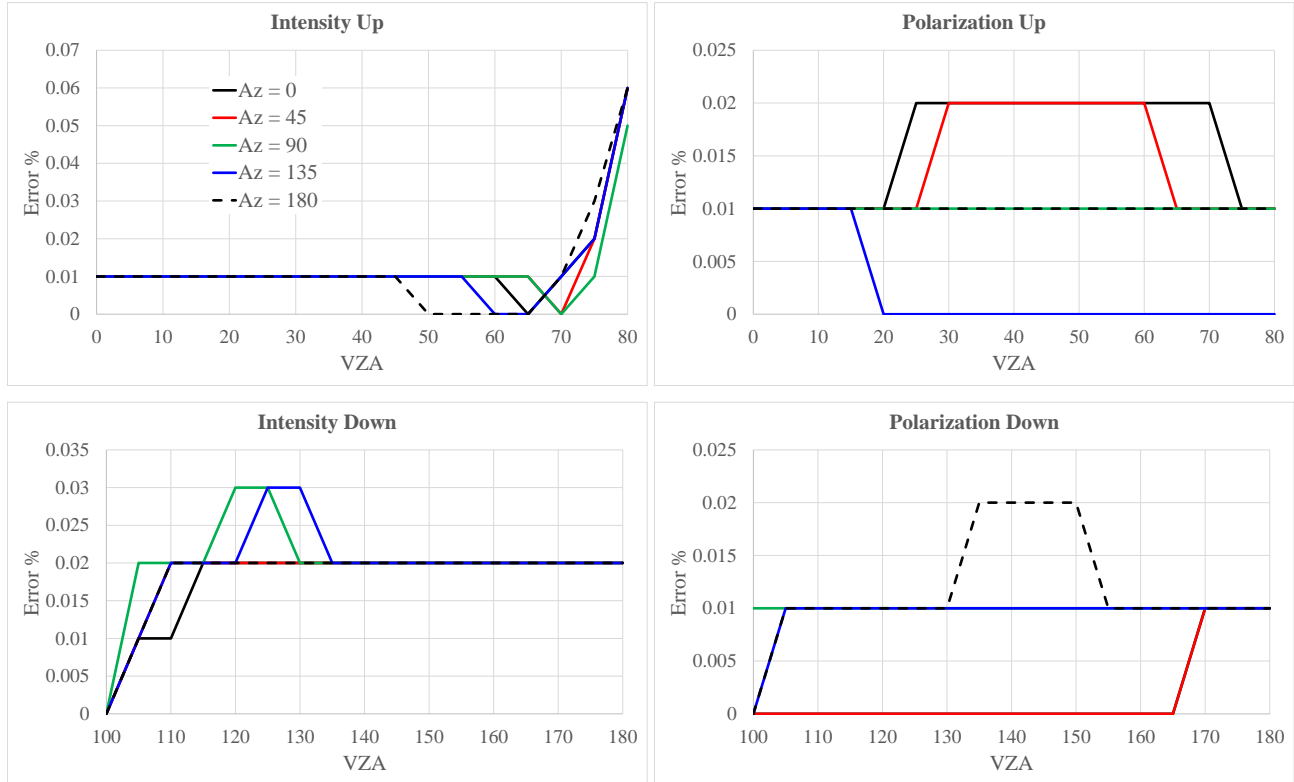


Figure 6. Relative deviation between SORD simulation of the IPRT case B2 and corresponding benchmark. Results are shown for intensity (left column) and polarization (right column) on TOA (top row) and BOA (bottom row), and different azimuths (in color). Az = 0° (solid black line) and 180° (dash black line) is the principal plane.

Finally, in Figure 7 we compare results of simulation using RT code SORD against benchmark result for the case IPRT-B3. In this case, Rayleigh and gas absorption are the same as in B2. In addition to that, spheroidal dust aerosol is added. The total (scattering + absorption) aerosol optical thickness profile is shown in Figure 5 (right), orange line. Aerosol single scattering albedo is 0.787581. The phase function peak value is about 560, average scattering cosine is 0.84. Figure 2 in the IPRT paper⁶ shows all elements of the phase matrix. Total aerosol optical thickness, $\tau_A = 0.2$.

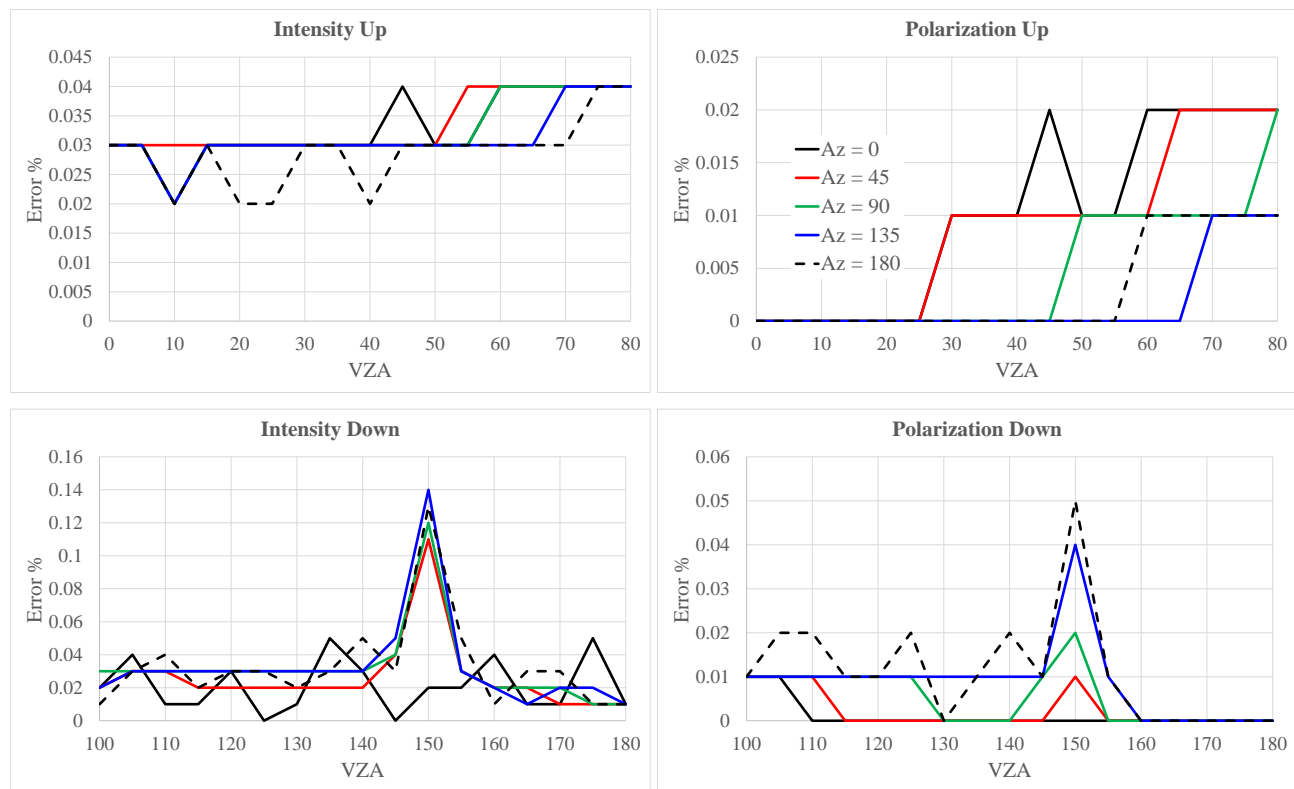


Figure 7. Same as in Figure 6, except for the IPRT-B3 scenario: aerosol profile.

In this case, one needs to apply the same subroutine GROUPTAU to aerosol scattering optical thickness as well as to the Rayleigh scattering thickness. This allows for computation of SSA in each optical layer, which comes on input for SORD. As in the case IPRT-B2, our agreement with the benchmark result meet the accuracy requirements defined in the Introduction. As expected, the highest discrepancy is observed at $VZA=180^\circ$ - $SZA=180^\circ-30^\circ=150^\circ$ only for $Az > 0$ (see Figure 7, Intensity Down and Polarization Down). This difference is due to Fourier summation over azimuth^{1,2,12}. It can be reduced, if needed, by taking more Fourier terms. Note that a widely used exact computation of the primary scattered radiation at the aureole area, $Az = 0$, makes the discrepancy negligible only at this azimuth angle.

3. CONCLUSION

This our paper finalizes validation of our new successive orders of scattering vector RT code SORD. We have considered cases of atmospheres with multiple layers and developed tools that conveniently integrate complicate atmospheric profiles into successive orders of scattering RT code. With these tools, we achieved good agreement with the benchmarks that mix Rayleigh, aerosol, and gas absorption components. In the IPRT cases B2 and B3, the observed error is at or below the level that is necessary for RT codes development and definitely within the desired range of measurement precision.

Nevertheless, for the almost conservative (SSA close to 1.0) IPRT case B4: Cloud bounded from either side by Rayleigh atmosphere, we found that even minor change in Rayleigh atmosphere profile causes significant deviation from published benchmark. This modification in Rayleigh profile is caused by integration over height used in the method of successive orders. Namely, if the simple yet accurate method of integration with equal step over optical thickness is used, the Rayleigh layers are combined and the profile is changed. If the method of successive orders of scattering is

used in such scenarios, one should consider using different types of integration techniques. For example, integration of the RT equation with a $d\tau$ -step unique in each optical layer¹³, or combination of numerical and analytical (semi-analytic) techniques¹⁴. These approaches are expected to increase accuracy. Unfortunately, the main advantage of the successive orders of scattering technique – simplicity – vanishes in these techniques.

Our code is publicly available as an open-source from http://maiac.gsfc.nasa.gov/pub/skorkin/SORD_IP_16B/ or by email request from the first author.

4. APPENDIX: SUBROUTINES FOR HEIGHT PROFILES

4.1 Computation of heights that split atmosphere into pieces with the same optical thickness

```
SUBROUTINE SPLITTAU(DTAU, NX, TAU, NL, ZKM, NZ, XKM)
!=====
! PURPOSE:
!   To compute heights, XKM, splitting the input Tau(z) into dTau-thick pieces
!
! INPUT:
!   DTAU  D(1)      Thickness between XKM(IX) & XKM(IX+1) (Increment)
!   NX    I(1)      Number of boundaries at the dTau-layers: sum(TAU)=dTau*(NX-1)
!   TAU   D(NL)     Thicknesses of each input layer
!   NL    I(1)      Number of input layers, NZ-1
!   ZKM   D(NZ)     Heights at Tau, from TOA to BOA: ZKM(I) > ZKM(I+1)
!   NZ    I(1)      Number of input heights, NL+1
!
! OUTPUT:
!   XKM   D(NX)     Heights, TOA to BOA, which split TAU with increment DTAU.
!                   Note, XKM(1) = ZKM(1) & XKM(NB) = ZKM(NZ)
!
! TREE:
!   -
!
! COMMENTS:
!   On input, the user must satisfy the following condition:
!
!       DTAU*(NX-1) = SUM(DTAU),
!
!   e.g. by doing DTAU=TAU0/CEILING(TAU0/DTAU). Here TAU0=SUM(TAU) and
!   CEILING(X) returns the least integer .ge. X [1].
!
!   There are only two possible cases. Case A: the current layer TAU(IL=IZ-1)
!   fits in the residual thickness entirely. Crop TAU(IL) from the residual, get
!   XKM(IX) and proceed to the next IX. Case B: there is at least one layer,
!   TAU(IL), between the known XKM(IX-1) and the next XKM(IX) which is yet to be
!   determined. Accumulate layer(s), TAU(IL), in this case. Note, the case
!   XKM(IX+1) = ZKM(IZ) falls under case A.
!
! REFERENCES:
!   1. https://gcc.gnu.org/onlinedocs/gfortran/CEILING.html#CEILING
!=====
!
IMPLICIT NONE
!
! INPUT VARIABLES
INTEGER, INTENT(IN) :: NX, NL, NZ
REAL*8, INTENT(IN) :: DTAU
```



```

!
! INPUT ARRAYS
  REAL*8, DIMENSION(NL), INTENT(IN) :: TAU
  REAL*8, DIMENSION(NZ), INTENT(IN) :: ZKM
!
! OUTPUT ARRAYS
  REAL*8, DIMENSION(NX), INTENT(OUT) :: XKM
!
! LOCAL VARIABLES
  INTEGER &
    IX, & ! Loop index over XKM
    IZ    ! Loop index over ZKM
  REAL*8 &
    EXT, & ! Extinction in the layer IL=IZ-1
    TACC, & ! Accumulated Tau
    TCOM, & ! Complimentary thickness, DTAU - TACC
    TRES    ! Residual thickness for the current layer IL=IZ-1
!=====
!
! TOA
  XKM(1) = ZKM(1)
!
! Internal XKM, if any
  IZ = 2
  EXT = TAU(1)/(ZKM(1) - ZKM(2))
  DO IX = 2, NX-1
    TRES = EXT*(XKM(IX-1) - ZKM(IZ))
    IF (TRES >= DTAU) THEN
!
!      Case A:
!      1. Residual of the layer IZ-1 is thick enough to hold dTau;
!      2. XKM(IX) belongs to the layer IZ-1, i.e. XKM(IX)>=ZKM(IZ);
!      3. Do not move ZKM(IZ) in this case;
!      4. Proceed to next XKM(IX) from the loop.
      XKM(IX) = XKM(IX-1) - DTAU/EXT
    ELSE ! TRES < DTAU
!
!      Case B:
!      1. Residual of the layer IZ-1 is thin;
!      2. Move ZKM(IZ) in this case;
!      3. Combine with the next layer(s) until thick enough;
!      4. XKM(IX) belongs to the layer that violates TACC < DTAU;
!      5. Complementary thickness, TCOM, is cropped from this layer;
!      6. TAU(IL=IZ-1) - TCOM becomes the residual thickness, TRES;
!      7. Extinction, EXT, is redefined:
!
!          EXT = TAU(IZ-1)/(ZKM(IZ-1) - ZKM(IZ))
!
!      8. Proceed to next XKM(IX) from the loop.
      TACC = TRES
      DO WHILE (TACC < DTAU)
        IZ = IZ+1 ! Take the next layer ...
        TACC = TACC + TAU(IZ-1) ! ... and keep accumulating
      END DO ! WHILE (TACC < DTAU)
      TACC = TACC - TAU(IZ-1) ! Overaccumulation: go one step back
      TCOM = DTAU - TACC ! Out of TAU(IZ-1) only TCOM is needed
      EXT = TAU(IZ-1)/(ZKM(IZ-1) - ZKM(IZ)) ! New extinction for Case A
      XKM(IX) = ZKM(IZ-1) - TCOM/EXT
    END IF
  END DO
!
!
!

```

```

        END IF ! TRES >= DTAU
    END DO ! IX = 2, NX-1
!
!   BOA
    XKM(NX) = ZKM(NZ)
!
END SUBROUTINE SPLITTAU

```

4.2 Redistribute optical thickness from the given input heights to the ones computed with SPLITTAU

SUBROUTINE GROUPTAU (NZ, ZKM, NL, TAU, NX, XKM, NG, TAUG)

```

!=====
! PURPOSE:
!   To rearrange the input TAU(ZKM) on a new grid, XKM
!
! INPUT:
!   NZ      I(1)      Number of heights for the input TAU
!   ZKM      D(NZ)     Heights for TAU, TOA to BOA; ZKM(1)=XKM(1) & ZKM(NZ)=XKM(NX)
!   NL      I(1)      Number of input layers, NZ-1
!   TAU      D(NL)     Thickness for each layer
!   NX      I(1)      Number of heights for the output TAUG
!   XKM      D(NX)     Heights for TAUG, TOA to BOA; XKM(1)=ZKM(1) & XKM(NX)=ZKM(NZ)
!   NG      I(1)      Number of output layers, NX-1
!
! OUTPUT:
!   TAUG      D(NG)     TAU(ZKM) rearranged according to XKM
!
! TREE:
!   -
!
! COMMENTS:
!   ZKM and XKM must coincide on TOA & BOA, respectively.
!
!   The idea is to compute contribution (weight) of each input layer TAU(IL),
!   located in ZKM(IL):ZKM(IL+1), to each output layer TAUG(IG), located in
!   XKM(IG):XKM(IG+1). There are 4 options:
!
!   Case 0: TAU(IL) & TAUG(IG) do not overlap - zero weight, W = 0
!   Case 1: TAU(IL) completely fits into TAUG(IG). W = 1.
!           XKM(IG) >= ZKM(IL) > ZKM(IL+1) >= XKM(IG+1)
!   Case 2: Opposite to Case 1, TAU(IG) completely fits into TAU(IL)
!           ZKM(IL) > XKM(IG) > XKM(IG+1) > ZKM(IL+1)
!           W = (XKM(IG) - XKM(IG+1))/DZ
!   Case 3: TAU(IL) partially overlaps TAU(IG) from the top
!           ZKM(IL) > XKM(IG) > ZKM(IL+1) > XKM(IG+1)
!           W = (XKM(IG) - ZKM(IL+1))/DZ
!   Case 4: TAU(IL) partially overlaps TAU(IG) from the bottom
!           XKM(IG) > ZKM(IL) > XKM(IG+1) >= ZKM(IL+1)
!           W = (ZKM(IL) - XKM(IG+1))/DZ
!
!   In Cases 1-4, DZ = ZKM(IL) - ZKM(IL+1).
!
!   TOP & BOT indices for IX & IZ are introduced for convenience only.
!
! REFERENCES:

```

```

! -
!=====
!
!   IMPLICIT NONE
!
! INPUT VARIABLES
!   INTEGER, INTENT(IN) :: NZ, NL, NX, NG
!
! INPUT ARRAYS
!   REAL*8, DIMENSION(NZ), INTENT(IN) :: ZKM
!   REAL*8, DIMENSION(NL), INTENT(IN) :: TAU
!   REAL*8, DIMENSION(NX), INTENT(IN) :: XKM
!
! OUTPUT ARRAYS
!   REAL*8, DIMENSION(NG), INTENT(OUT) :: TAUG
!
! LOCAL VARIABLES
!   INTEGER &
!       IG,           & ! Loop index over TAUG(IG) ("steady" layer)
!       IL,           & ! Loop index over TAU(IL) ("moving" layer)
!       IX_TOP, IX_BOT, & ! Define position of TAUG(IG)
!       IZ_TOP, IZ_BOT  ! Define position of TAU(IL)
!=====
!
!   DO IG = 1, NG-1
!       IX_TOP = IG
!       IX_BOT = IG+1
!       TAUG(IG) = 0.0D0 ! Initialize & account for non-overlapping layers
!       DO IL = 1, NL
!           IZ_TOP = IL
!           IZ_BOT = IL+1
!           IF (ZKM(IZ_TOP) <= XKM(IX_TOP) .AND. &
!               ZKM(IZ_BOT) >= XKM(IX_BOT)) THEN ! Case (1)
!               TAUG(IG) = TAUG(IG) + TAU(IL)
!           ELSE IF (ZKM(IZ_TOP) > XKM(IX_TOP) .AND. &
!                   ZKM(IZ_BOT) < XKM(IX_BOT)) THEN ! Case (2)
!               TAUG(IG) = TAUG(IG) + TAU(IL)*(XKM(IX_TOP) - XKM(IX_BOT))/ &
!                   (ZKM(IZ_TOP) - ZKM(IZ_BOT))
!           ELSE IF (ZKM(IZ_TOP) > XKM(IX_TOP) .AND. &
!                   ZKM(IZ_BOT) < XKM(IX_TOP)) THEN ! Case (3)
!               TAUG(IG) = TAUG(IG) + TAU(IL)*(XKM(IX_TOP) - ZKM(IZ_BOT))/ &
!                   (ZKM(IZ_TOP) - ZKM(IZ_BOT))
!           ELSE IF (ZKM(IZ_TOP) > XKM(IX_BOT) .AND. &
!                   ZKM(IZ_BOT) < XKM(IX_BOT)) THEN ! Case (4)
!               TAUG(IG) = TAUG(IG) + TAU(IL)*(ZKM(IZ_TOP) - XKM(IX_BOT))/ &
!                   (ZKM(IZ_TOP) - ZKM(IZ_BOT))
!           END IF ! Cases 1-4
!       END DO ! IL = 1, NL
!   END DO ! IG = 1, NG-1
!
!   TAUG(NG) = SUM(TAU) - SUM(TAUG(1:NG-1))
!
! END SUBROUTINE GROUPTAU

```

ACKNOWLEDGEMENTS

This research is supported by the NASA ROSES-14 program “Remote Sensing Theory for Earth Science” managed by Dr. Lucia Tsaoussi, grant number NNX15AQ23G.

REFERENCES

- [1] van de Hulst, H. C., [Multiple light scattering. Tables, formulas, and applications], Academic Press, New York (1980). Volume 1, Section 4.3, p.46;
- [2] Lenoble, J. (Ed.), [Radiative Transfer in Scattering and Absorbing Atmospheres: Standard Computational Procedures], A. Deepak Publishing, Hampton VA (1985), Section 3.7, p.46;
- [3] Korkin, S., Lyapustin A., Sinyuk, A., and Holben, B., “A new code SORD for simulation of polarized light scattering in the Earth atmosphere”, Proc. SPIE 9853, Polarization: Measurement, Analysis, and Remote Sensing XII, 985305, DOI: 10.1117/12.2223423. <http://spie.org/Publications/Proceedings/Paper/10.1117/12.2223423>
- [4] Holben, B. N., Eck, T. F., Slutsker, I., Tanré, D., Buis, J. P., Setzer, A., Vermote, E., Reagan, J. A., Kaufman, Y. J., Nakajima, T., Lavenu, F., Jankowiak, I., and Smirnov, A., “AERONET-A Federated instrument Network and Data Archive for Aerosol Characterization”, Rem. Sens. Env. 66, 1–16 (1998).
- [5] Dubovik, O., Herman, M., Holdak, A., Lapyonok, T., Tanré, D., Deuzé, J. L., Ducos, F., Sinyuk, A., Lopatin, A., “Statistically optimized inversion algorithm for enhanced retrieval of aerosol properties from spectral multi-angle polarimetric satellite observations”, Atmos. Meas. Tech. 4, 975–1018 (2011).
- [6] Emde, C., Barlas, V., Cornet, C., Evans, F., Korkin, S., Ota, Y., C-Labonnote, L., Lyapustin, A., Macke, A., Mayer, B., and Wendisch, M., “IPRT polarized radiative transfer model intercomparison project – Phase A”, J. Quant. Spect. Rad. Trans. 164, 8-36 (2015).
- [7] Lenoble, J., Herman, M., Deuzé, J L., Lafrance, B., Santer, R., and Tanré, D., “A successive order of scattering code for solving the vector equation of transfer in the earth’s atmosphere with aerosols”, J. Quant. Spect. Rad. Trans. 107, 479-507 (2007).
- [8] Dubovik, O., Lapyonok, T., Litvinov, P., Herman, M., Fuertes, D., Ducos, F., Lopatin, A., Chaikovsky, A., Torres, B., Derimian, Y., Huang, X., Aspetsberger, M., and Federspiel, C., “GRASP: a versatile algorithm for characterizing the atmosphere”, SPIE: Newsroom, DOI:10.1117/2.1201408.005558, Published Online: September 19, 2014. <http://spie.org/x109993.xml> (16 March 2016).
- [9] Mishchenko, M. I., “The fast invariant imbedding method for polarized light: computational aspects and numerical results for Rayleigh scattering”, J. Quant. Spect. Rad. Trans. 43(2), 163-171 (1990).
- [10] Diner, D. J., Davis, A., Hancock, B., Gutt, G., Chipman, R. A., and Cairns, B., “Dual-photoelastic-modulator-based polarimetric imaging concept for aerosol remote sensing”, Appl. Opt. 46(35), 8428-8445 (2007).
- [11] Hasekamp, O. P., and Landgraf, J., “Retrieval of aerosol properties over land surfaces: capabilities of multiple-viewing-angle intensity and polarization measurements”, Appl. Opt. 46(16), 3332-3344 (2007).
- [12] Hovenier, J.W., van der Mee C., and Domke H., [Transfer of polarized light in planetary atmospheres. Basic concepts and practical methods], Kluwer Academic Publishers, Dordrecht, Netherlands (2004).
- [13] Zhai, P.-W., Hu, Y., Chowdhary, J. C., Trepte, C. R., Lucker, P. L., and Josset D. B., “A vector radiative transfer model for coupled atmosphere and ocean systems with a rough surface”, J. Quant. Spect. Rad. Trans. 111, 1025-1040 (2010).
- [14] Duan, M. and Min, Q., “A semi-analytic technique to speed up successive order of scattering model for optically thick media”, J. Quant. Spect. Rad. Trans. 95, 21-32 (2005).